BLOOD VESSEL SEGMENTATION FROM COLOR RETINAL IMAGES USING UNSUPERVISED TEXTURE CLASSIFICATION

Alauddin Bhuiyan, Baikunth Nath, Joselito Chua and Ramamohanarao Kotagiri

Computer Science and Software Engineering, The University of Melbourne, Australia.
{bhuiyanm, bnath, jjchua, rao} @csse.unimelb.edu.au

ABSTRACT

Automated blood vessel segmentation is an important issue for assessing retinal abnormalities and diagnoses of many diseases. The segmentation of vessels is complicated by huge variations in local contrast, particularly in case of the minor vessels. In this paper, we propose a new method of texture based vessel segmentation to overcome this problem. We use Gaussian and $L^*a^*b^*$ perceptually uniform color spaces with original RGB for texture feature extraction on retinal images. A bank of Gabor energy filters are used to analyze the texture features from which a feature vector is constructed for each pixel. The Fuzzy C-Means (FCM) clustering algorithm is used to classify the feature vectors into vessel or non-vessel based on the texture properties. From the FCM clustering output we attain the final output segmented image after a post processing step. We compare our method with hand-labeled ground truth segmentation of five images and achieve 84.37% sensitivity and 99.61% specificity.

Index Terms— Medical Image, texture classification, Gabor energy filter bank, FCM clustering, image segmentation

1. INTRODUCTION

The automatic detection of blood vessels is very important as ophthalmologists can potentially screen larger populations for vessel abnormalities. In contrast, manual delineation of vessels becomes tedious or even impossible when the number of vessels in an image is large or when a large number of images are acquired. Blood vessel appearance can provide information on pathological changes caused by some diseases including diabetes, hypertension, and arteriosclerosis. Changes in retinal vasculature, such as hemorrhages, angiogenesis; increases in vessel tortuosity, blockages and arteriolar-venular diameter ratios are important indicators of, for example, diabetic retinopathy, and retinopathy of prematurity and cardiovascular risk. Information about blood vessels in retinal images can be used in grading disease severity or as part of the process of automated diagnosis of diseases [1].

Automated retinal segmentation is complicated by the fact that the width of the retinal vessels can vary from large to very small, and the local contrast of vessels is unstable, especially in unhealthy retinal images. Although a large number of schemes [1, 2, 3, 4, 5] have been proposed for the detection of blood vessels, a huge improvement in detection procedures remains a necessity for the detection of minor vessels. So far, the maximum detection rate achieved 94.4% overall [3] and for minor vessels it is only 75% [4].

In this paper we propose a novel approach for vessel segmentation which is equally efficient to detect major and minor vessels. We consider Gaussian and $L^*a^*b^*$ perceptually uniform color spaces with the original RGB image for texture feature extraction. To extract features, a bank of Gabor energy filters with three wavelengths and twenty-four orientations is applied in each selected color channel. Then a texture image is constructed from the maximum response of all orientations for a particular wavelength in each color channel. From the texture images, a feature vector is constructed for each pixel. These feature vectors are classified using the FCM clustering algorithm. Finally, we segment the image based on the cluster centroid value.

The rest of the paper is organized as follows: Section 2 introduces our proposed method of blood vessel segmentation using unsupervised texture classification. Image color space transformation and preprocessing technique are described in section 3. Section 4 and 5 illustrate texture analysis and classification procedure. The overall results are provided in section 6 and finally conclusion and future research directions are drawn in section 7.

2. PROPOSED METHOD

We propose a method for blood vessel segmentation which is based on the texture property analysis of vessel and non vessel parts in the color retinal images. The reasons are as follows. Firstly, due to large variation of local contrast in the retinal image, texture analysis is more appropriate to extract features from vessel and non vessel parts in the retinal images. Secondly, a color texture is a spatio-chromatic pattern and can be defined as the "distribution of colors over a surface"; therefore, incorporating color into texture analysis is enhancing the procedure. The original retinal images are in RGB color space which is not perceptually uniform and Euclidean distances in 3D RGB space do not correspond to color

differences as perceived by humans. In addition, perceptually uniform color spaces are very effective in rotation invariant color texture analysis. So, we use perceptually uniform color spaces along with original RGB color channels to extract texture features.

At first we apply the transformation of original RGB image into Gaussian and $L^*a^*b^*$ color space. We choose first two components of Gaussian color space $\hat{E}$ and $\hat{E_\lambda}$, Luminance L from $L^*a^*b^*$ color space and Green channel G from RGB color space due to the higher contrast of vessel and background which is convenient for texture analysis. We apply Adaptive Histogram Equalization (AHE) method to these four different color channel images for contrast enhancement. For each of these color channels, we apply a bank of Gabor filters with twenty-four orientations and three wavelengths for texture feature extraction. We construct the texture image in each color channel for every wavelength considering the maximum response of all twenty-four orientations. These texture images are used to analyze the number of clusters which latter will be used as the classifier input. Consequently, we construct twelve texture images for each original retinal image. We construct a feature vector for every pixel mapping each pixel position of all these texture images (i.e. each feature vector is in the length of twelve elements). These feature vectors are classified as a vessel or background part using unsupervised FCM clustering algorithm. From the output of the FCM clustering algorithm we construct a 2D matrix (as original image dimension) with cluster numbers which have the highest membership values (for each position). Finally, we produce the ultimate segmented image with converting the cluster numbers into binary values considering the cluster centroid values. Figure 1 portrays the overall technique of our proposed method.

3. COLOR SPACE TRANSFORMATION AND PREPROCESSING

Generally image data is given in RGB space (because of the availability of data produced by the camera apparatus). The definition of $L^*a^*b^*$ is based on an intermediate system, known as the CIE XYZ space (ITU-Rec 709). This space is derived from RGB as below [6]

$$\begin{aligned} X &= 0.412453R + 0.357580G + 0.180423B \\ Y &= 0.212671R + 0.715160G + 0.072169B \\ Z &= 0.019334R + 0.119193G + 0.950227B \end{aligned} \tag{1}$$

$L^*a^*b^*$ color space is defined as follows:

$$\begin{aligned} L^* &= 116f(Y/Y_n) - 16 \\ a^* &= 500[f(X/X_n) - f(Y/Y_n)] \\ b^* &= 200[f(Y/Y_n)] - f(Z/Z_n) \end{aligned} \tag{2}$$

where $f(q) = q^{1/3}$ if $q < 0.008856$ otherwise $f(q) = 7.87 + 16/116$. X_n, Y_n and Z_n represent a reference white as defined by a CIE standard illuminant, D_{65} in this case. This

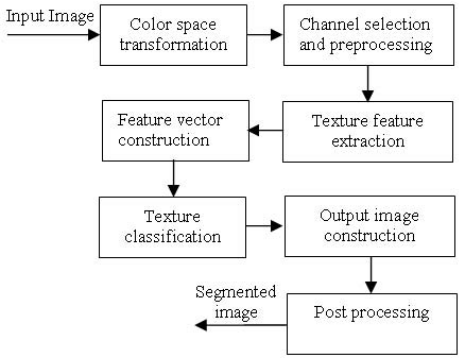

Fig. 1. The vessel segmentation model.

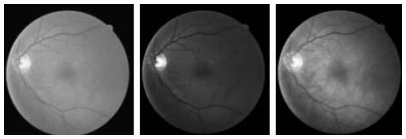

Fig. 2. Original RGB image and Gaussian transformed first and second component image (left to right).

is obtained by setting $R = G = B = 100$ in (1), $q \in \{X/X_n, Y/Y_n, Z/Z_n\}$. Gaussian color model can also be well approximated by the RGB values. The first three components $\hat{E}$, $\hat{E_\lambda}$ and $\hat{E_{\lambda\lambda}}$ of the Gaussian color model (Taylor expansion of the Gaussian weighted spectral energy distribution at Gaussian central wavelength and scale) can be approximated from the CIE 1964 XYZ basis when taking $\lambda_0 = 520nm$ (Gaussian central wavelength) and $\sigma_\lambda = 55nm$ (scale) as follows [7]

$$\begin{pmatrix} \hat{E} \\ \hat{E_\lambda} \\ \hat{E_{\lambda\lambda}} \end{pmatrix} = \begin{pmatrix} -0.48 & 1.2 & 0.28 \\ 0.48 & 0-0.4 & -0.4 \\ 1.18 & -1.3 & 0 \end{pmatrix} \begin{pmatrix} X \\ Y \\ Z \end{pmatrix} \tag{3}$$

The product of (1) and (3) gives the desired implementation of the Gaussian color model in RGB terms (Fig. 2). The Adaptive Histogram Equalization method was implemented, using MATLAB, to enhance the contrast of the image intensity by transforming the values using contrast-limited adaptive histogram equalization (Fig. 3).

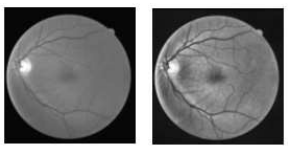

Fig. 3. Retinal Green channel image in figure 2 (left) and its AHE filtered image (right).

4. TEXTURE FEATURES EXTRACTION

Texture generally describes second order property of surfaces and scenes, measured over image intensities. A Gabor filter has weak responses along all orientations on the smooth (background) surface. On the other hand, when it positioned on a linear pattern object (like a vessel) the Gabor filter produces relatively large differences in its responses when the orientation parameter changes [4]. Hence, the use of Gabor filters to analyze the texture of the retinal images is very promising. In the following two subsections we illustrate the Gabor filter based texture analysis method.

4.1. Gabor Filter

An input image $I(x, y)$, $(x, y) \in \Omega$ where Ω is the set of image points, is convolved with a 2D Gabor function $g(x, y)$, $(x, y) \in \omega$, to obtain a Gabor feature image $r(x, y)$ (Gabor filter response) as follows [8]

$$r(x,y) = \iint_{\Omega} I(\xi,\eta) g(x-\xi, y-\eta) d\xi d\eta \tag{4}$$

We use the following family of 2D Gabor functions to model the spatial summation properties of an image [8]

$$\begin{array}{c} g_{\xi,\eta,\lambda,\Theta,\phi}(x,y) = \exp(-\frac{x'^2+\gamma^2 y'^2}{2\sigma^2}) \cos(2\pi \frac{x'}{\lambda} + \phi) \\ x' = (x-\xi)\cos\Theta - (y-\eta)\sin\Theta \\ y' = (x-\xi)\cos\Theta - (y-\eta)\sin\Theta \end{array} \tag{5}$$

where the arguments x and y specify the position of a light impulse in the visual field and $\xi, \eta, \sigma, \gamma, \lambda, \Theta, \phi$ are parameters. The pair (ξ, η) specifies the center of a receptive field in image coordinates. The standard deviation σ of the Gaussian factor determines the size of the receptive filed. Its eccentricity and herewith the eccentricity of the receptive field ellipse is determined by the parameter γ called the spatial aspect ratio. This ratio is known to vary in a limited range of $0.23 < \gamma < 0.92$. We used $\gamma = 0.5$ for our simulation. The parameter λ is the wavelength of the cosine factor which determines the preferred spatial frequency $\frac{1}{\lambda}$ of the receptive field function $g_{\xi,\eta,\lambda,\Theta,\phi}(x, y)$. The ratio σ/λ determines the spatial frequency bandwidth of a linear filter based on the function g. The parameter Θ specifies the orientation of the normal to the parallel excitatory and inhibitory stripe zones - this normal is the axis x' in (5). Finally, the parameter $\phi \in (-\pi, \pi)$, which is a phase offset argument of the harmonic factor $\cos(2\pi \frac{x'}{\lambda} + \phi)$, determines the symmetry of the function $g_{\xi,\eta,\lambda,\Theta,\phi}(x, y)$. For $\phi = 0$ and $\phi = \pi$ it is symmetric with respect to the center (ξ, η) of the receptive field; for $\phi = -\frac{1}{2}\pi$ and $\phi = \frac{1}{2}\pi$, the function is antisymmetric and all other cases are asymmetric mixture of these two. In our simulations we used $\phi = 0$ and $\phi = \frac{1}{2}\pi$.

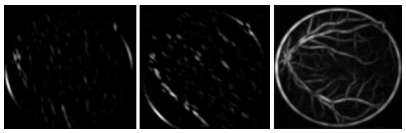

Fig. 4. Texture analyzed image with the orientations of 15, 45 degrees and maximum response of all twenty-four orientations (left to right).

4.2. Gabor Energy Features

A set of textures was obtained based on the use of Gabor filters (4) according to a multichannel filtering scheme. For this purpose, each image was filtered with a set of Gabor filters with different preferred orientation, spatial frequencies and phases. The filter results of the phase pairs were combined, yielding the Gabor energy quantity [8]:

$$E_{\xi,\eta,\Theta,\lambda} = \sqrt{r^2_{\xi,\eta,\Theta,\lambda,0} + r^2_{\xi,\eta,\Theta,\lambda,\pi/2}} \tag{6}$$

where $r^2_{\xi,\eta,\Theta,\lambda,0}$ and $r^2_{\xi,\eta,\Theta,\lambda,\pi/2}$ are the outputs of the symmetric and antisymmetric filters. We used Gabor energy filters with twenty-four equidistant preferred orientations ($\Theta = 0, 15, 30, .., 345$) and three preferred spatial frequencies ($\lambda = 6, 7, 8$). In this way an appropriate coverage was performed of the spatial frequency domain.

We considered the maximum response value per pixel on each color channel to reduce the feature vector length and complexity of training on data for the classifier. In addition, we constructed an image (Fig. 4) on each color channel which was used for histogram analysis to determine the cluster number. From these images we constructed twelve element length feature vector for each pixel in each retinal image to classify them into vessel and non-vessel using the FCM clustering algorithm.

5. TEXTURE CLASSIFICATION AND IMAGE SEGMENTATION

The FCM is a data clustering technique where in each data point belongs to a cluster to some degree that is specified by a membership grade. Let $X = x_1, x_2, , x_N$ where $x \in R^N$ present a given set of feature data. The objective of the FCM clustering algorithm is to minimize the Fuzzy C-Means cost function formulated as [9]

$$J(U,V) = \sum_{j=1}^{C} \sum_{i=1}^{N} (\mu_{ij})^m ||x_i - v_j||^2 \tag{7}$$

$V = \{v_1, v_2, , v_C\}$ are the cluster centers. $U = (\mu_{ij})_{N\times C}$ is fuzzy partition matrix, in which each member is between the data vector x_i and the cluster j. The values of matrix U should satisfy the following conditions:

$$\mu_{ij} \in [0,1], \forall i = 1, .., N, \forall j = 1, .., C \tag{8}$$

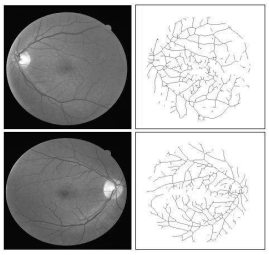

Fig. 5. Original image (left) and segmented vessel centerline images (right).

$$\mu_{ij} = 1, \forall i = 1, .., N \tag{9}$$

The exponent $m \in [1, \infty]$ is the weighting exponent, which determines the fuzziness of the clusters. The most commonly used distance norm is the Euclidean distance $d_{ij} = ||x_i - v_j||$.

We used the Matlab Fuzzy Logic Toolbox for clustering 253440 vectors (the size of the retinal image is 512x495) in length twelve for each retinal image. In each retinal image clustering procedure, the number of clusters was assigned after analyzing the histogram of the texture image. The parameter values used for the FCM clustering were as follows. The exponent value of 2 for the partition matrix, maximum number of iterations was set to 1000 for the stopping criterion and the minimum amount of improvement being 0.00001. We received the membership values on each cluster for every vector, from which we picked the cluster number that belonged to the highest membership value for each vector and converted it into a 2D matrix. From this matrix we produced the binary image considering the cluster central intensity value which identifies the blood vessels only.

6. EXPERIMENTAL RESULTS

Using the DRIVE database [10] we applied our method for vessel segmentation. For performance evaluation, we detected the vessel centerline in our output segmented images and hand-labeled ground truth segmented (GT) images applying the morphological thinning operation (Fig. 5). We did not compare the segmented images directly with the GT images as the vessel width in the GT images were not always accurate although the vessel position were proper (also reported in [1]). In our experiment, we compared five skeletonized images of our method with the GT images. We assumed that the maximum centerline movement on the GT images is two pixels. A pixel on centerline is considered positive and a background pixel is negative. We achieved an overall 84.37% sensitivity and 99.61% specificity. Hoover et al. [1] method on the same five segmented images resulted in 68.23% sensitivity and 98.06% specificity. Clearly, our method produces superior results.

7. CONCLUSION AND FUTURE WORK

In this paper we proposed a novel approach for a texture based vessel segmentation technique. Our method is very efficient in detecting both major and minor blood vessels. Currently, we are working on the segmented images to measure vessel width and vessel bifurcation and crossover detection.

8. REFERENCES

[1] A. Hoover, V. Kouznetsova, and M. Goldbaum, "Locating blood vessels in retinal images by piece-wise threshold probing of a matched filter response," *IEEE Transactions on Medical Imaging*, vol. 19(3), pp. 203–210, 2000.

[2] A. M. Mendonca and A. Campilho, "Segmentation of retinal blood vessels by combining the detection of centerlines and morphological reconstruction," *IEEE Transactions on Medical Imaging*, vol. 25(9), pp. 1200–1213, 2006.

[3] J. Staal, M. D. Abramoff, M. Niemeijer, M. A. Viergever, and B. V. Ginneken, "Ridge-based vessel segmentation in color images of the retina," *IEEE Transactions on Medical Imaging*, vol. 23(4), pp. 501–509, 2004.

[4] D. Wu, M. Zhang, and J. Liu, "On the adaptive detetcion of blood vessels in retinal images," *IEEE Transactions on Biomedical Engineering*, vol. 53(2), pp. 341–343, 2006.

[5] X. Jiang and D. Mojon, "Adaptive local thresholding by verification-based multithreshold probing with application to vessel detection in retinal images," *IEEE Transactions on Pattern Analysis and Machine Intelligence*, vol. 25(1), pp. 131–137, 2003.

[6] G. W. Wyszecki and S. W. Stiles, "Color science: Concepts and methods, quantitative data and formulas," *New York, Wiley*, 1982.

[7] J. Geusebroek, R. V. D. Boomgaard, A. W. M. Smeulders, and H. Geerts, "Color invariance," *IEEE Transactions on Pattern Analysis and Machine Intelligence*, vol. 23(2), pp. 1338–1350, 2001.

[8] P. Kruizinga and N. Petkov, "Nonlinear operator for oriented texture," *IEEE Transactions on Image Processing*, vol. 8(10), pp. 1395–1407, 1999.

[9] J. Bezdek, "Pattern recognition with fuzzy objective function algorithms," *Plenum Press, USA*, 1981.

[10] "The drive database," Image Sciences Institute, University Medical Center Utrecht, The Netherlands. http://www.isi.uu.nl/Research/Databases/DRIVE/.